Penerbit Akademia Baru

Malaysian Journal on Composites Science and Manufacturing

Journal homepage:
https://www.akademiabaru.com/submit/index.php/mjcsm/
ISSN: 2716-6945

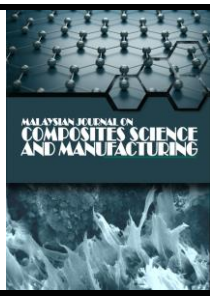

Effect of Metal Filler on the Welded Joint of X70 Steel Joined to Duplex Stainless Steel by Gas Arc Welding

Open Access

Zakaria Bourmerzoug[1, *], Oualid Beziou[1], Ines Hamdi[2], François Brisset[3], Thierry Baudin[3]

[1] Mechanical Engineering Department, LMSM Laboratory, Biskra University, Algeria.
[2] Chemical Engineering Department, LMSM Laboratory, Biskra University, Algeria.
[3] Université Paris-Saclay, CNRS, Institut de Chimie Moléculaire et des Matériaux d'Orsay, 91405 Orsay, France

ARTICLE INFO

Article history:
Received 4 November 2024
Received in revised form 16 February 2025
Accepted 24 February 2025
Available online 30 March 2025

Keywords:
Arc welding, Filler, Dissimilar steels, Microstructures, Mechanical properties, Corrosion resistance

ABSTRACT

This study investigates the effects of using two different metal fillers on the microstructure, corrosion resistance, and mechanical properties of a duplex stainless steel and X70 steel welded joint, performed using the Gas Tungsten Arc Welding (GTAW) process. The electrodes employed were ER2209 and ER70S. The research aims to assess the feasibility of welding dissimilar steels with these two electrodes. Three weld passes were conducted using the different electrodes, followed by characterization of the welded joint's microstructure and evaluation of its mechanical properties. The primary characterization techniques included optical microscopy, scanning electron microscopy, Electron Backscatter Diffraction (EBSD), corrosion testing, Vickers microhardness, and tensile testing. The welded joint exhibited no visible defects, and using two electrodes increased the hardness, particularly in the fusion zone, where it reached 290 HV. Microscopic analysis revealed a solidification microstructure in the fusion zone. The welded joint demonstrated intermediate corrosion resistance between the two base steels (duplex stainless steel and X70). At the same time, its tensile strength was also intermediate, achieving more than 96% of the nominal tensile strength of duplex stainless steel. This approach of bonding dissimilar steels offers a potential solution for substituting one steel type with another in automotive structures, enhancing their resistance and reducing production costs.

**Corresponding author.*
E-mail address: z.boumerzoug@univ-biskra.dz (Zakaria Boumerzoug)
Email of co-authors: bezziouwalid@gmail.com , ines.hamdi@univ-biskra.dz , francois.brisset@universite-paris-saclay.fr , thierry.baudin@universite-paris-saclay.fr

https://doi.org/10.37934/mjcsm.16.1.1934

1. Introduction

Welding is a widely used joining process in various industries, including automotive, shipbuilding, and pipeline construction. From a metallurgical perspective, a welded joint typically consists of three distinct zones. The first is the fusion zone (FZ), the central area where the electrode fuses with the base metal. The second is the heat-affected zone (HAZ), which is influenced by the heat from the fusion zone. The third is the base material (BM), which remains unaffected by the thermal cycle [1].

In pipeline construction for hydrocarbon transportation, welding different steels, such as X70 steel and duplex stainless steel, is common. X70 steel is a low-carbon steel composed of a ferritic matrix and pearlite colonies, while duplex stainless steel consists of both ferrite and austenite phases. Typically, pipelines are constructed using tubes made of the same type of steel, and an electrode with similar metallurgical properties as the base metal is selected. However, when welding dissimilar steels, choosing the optimal filler electrode becomes a challenge. This issue has prompted extensive research in recent years. As reported, the incorporation of efficient and high-quality welding processes for dissimilar metals is critical in power plants and transportation systems [2-3]. Welding two dissimilar ferrous metals involves using different base metals and filler metals [4].

Welding dissimilar steels presents several challenges due to the varying chemical, mechanical, and physical properties of the base metals. For example, Kaewkuekool and Amornsin [5] investigated the effects of gas metal arc welding (GMAW) parameters on the mechanical properties of dissimilar joints between AISI 304 stainless steel and low-carbon steel. They found that the type of filler metal significantly influenced the elongation and ultimate tensile strength of the welded joint. Mendoza et al. [6] examined the mechanical behavior of dissimilar welded joints between super duplex stainless steel and high-strength low-alloy steel, discovering that the use of the ER 25.10.4L filler metal resulted in mechanical properties superior to those of high-strength low-alloy steel in its as-received condition. The selection of a suitable consumable is typically based on the need to achieve a weld metal strength that exceeds the strength of the weaker parent material.

The welding of duplex stainless steels to other steels has attracted significant attention. Zahraei *et al.* [7] studied the influence of heat input in shielded arc welding on the microstructure of the heat-affected zone (HAZ) in dissimilar joints between API 5L X80 steel and DS5 2205 duplex stainless steel. They reported no defects, such as cracks, in the HAZ across all heat inputs. McPherson *et al.* [8] examined submerged arc welding of duplex stainless steel to carbon steel plates, identifying the presence of martensite but no significant carbide precipitation. Wang et al. [9] evaluated the quality of dissimilar weld joints between UNS S31803 duplex stainless steel and API X70 low-alloy steel using ER2209 welding wire with both GTAW and GMAW processes. They observed more severe corrosion at the fusion zone of the GTAW sample compared to the GMAW sample. Puchianu *et al.* [10] investigated the effects of Metal Active Gas (MAG) welding on dissimilar joints between high-strength steel and duplex stainless steel. Their mechanical testing results indicated that careful selection of gas type, filler material, and welding parameters resulted in welded joints with acceptable mechanical properties. Eghlimi *et al.* [11] studied the microstructure and texture evolution in dissimilar welded joints between super duplex stainless steel and high-strength low-alloy steel, finding that texture was primarily influenced by unidirectional solidification and competitive phase growth in the weld.

Recent studies have focused on the welding of X70 steel with duplex stainless steel using a single electrode, observing a solidification microstructure in the fusion zone, which was harder than both the heat-affected zone (HAZ) and the base metals [12]. These previous studies indicate that while duplex stainless steel can be welded to a limited range of steels, typically, only one filler material is

used to achieve the dissimilar joint. Further research is needed to explore the corrosion behavior and texture of such joints.

The present work investigates the effect of filler material on the microstructure, corrosion resistance, and mechanical properties of dissimilar welded joints between X70 steel and duplex stainless steel, welded using the Gas Tungsten Arc Welding (GTAW) process. Two different electrodes were used for welding: ER2209, typically employed for duplex stainless steels, and ER70S, often used for mild and medium-strength steels. This combination of two electrodes aims to produce a weld joint with optimal mechanical properties, a technique that has not been explored in previous studies.

2. Methodology

The base metals studied in this investigation are low carbon steel (X70) and duplex stainless steel, which are widely used in the construction of pipelines for transporting oil and gas. These steel tubes were made by 12 mm thick sheets. Table 1 presents the nominal chemical composition of these steels.

Table 1
Nominal chemical composition (Wt. %) of the base metals (X70 steel and duplex stainless steel)

Steel	Fe	C	Si	Mn	Cr	P	Mo	Ni	Other elements
X70	98.00	0.07	0.20	1.02	0.05	0.02	0.15	0.06	0.43
DSS	67.00	0.02	1.50	1.54	20.0	0.02	2.01	6.65	1.26

To ensure a good weld joint, a V-shaped butt weld was prepared. Two filler metals were used. Three passes were applied: the first is ER2209, and the second is ER70S. The ER2209 is used for the first and third passes and the ER70S for the second pass. The ER2209 electrode is used for welding duplex stainless steels and has high tensile strength and stress corrosion cracking resistance. On the other hand, the ER70S electrode is manufactured from a low-carbon steel wire and is used for welding mild and medium strength steels. The chemical of the two electrodes are presented in Tables 2 and 3. Table 4 gathers the welding parameters of the two dissimilar steels.

Table 2
Nominal chemical composition (Wt. %) of the electrode ER2209

Fe	C	Si	Mn	P	Cr	Ni	Mo	Cu	N	Co
62.88	0.01	0.48	1.50	0.02	23.00	8.60	3.20	0.10	0.15	0.06

Table 3
Nominal chemical composition (Wt. %) of the electrode ER70S

C	Si	Mn	P	Cr	Ni	Mo	Cu	V	Al	S
0.06	0.6	1.1	0.008	0.12	0.03	0.01	0.05	0.01	0.12	0.009

Table 4
Welding parameters of the two dissimilar steels

Parameter	Values
Filler diameter (mm)	2.4 mm
Current type	DC (-)
Voltage(V)	First pass: 10, Second and third passes: 19
Intensity (A)	100
Welding speed (cm/min)	First pass 5. Second and third passes: 10
Shielding gas	100 % *Ar*
Gas Flow (L/min)	18

For the microstructural investigations, the samples were cut perpendicularly to the welding direction corresponding to Transverse Direction (TD) (Figure 1). The main coordinate system of the rolled sheets *i.e. Rolling Direction* (RD), *Transverse Direction* (TD) and *Normal Direction* (ND) are indicated in Figure 1. The samples were polished with abrasive papers of different grits and then finished with a 3 µm diamond paste. As two different steels are used, the X70 steel was chemically etched with 2% Nital and the duplex stainless steel with a chemical solution of 5 g $CuCl_2$, 100 ml HCl, and 100 ml alcohol. The welded area was etched with 2% Nital.

For EBSD measurements, the standard sample preparation method was used, namely mechanical polishing, followed by OPS polishing of the sample cross-section. For the analysis of the EBSD results, a Zeiss Supra 50 FEG-SEM operating at 20 kV coupled with the OIM^{TM} (Orientation Imaging Microscopy) software belonging to the company TSL-EDAX was used. Figure 1 shows the schematic representation of the welded joint.

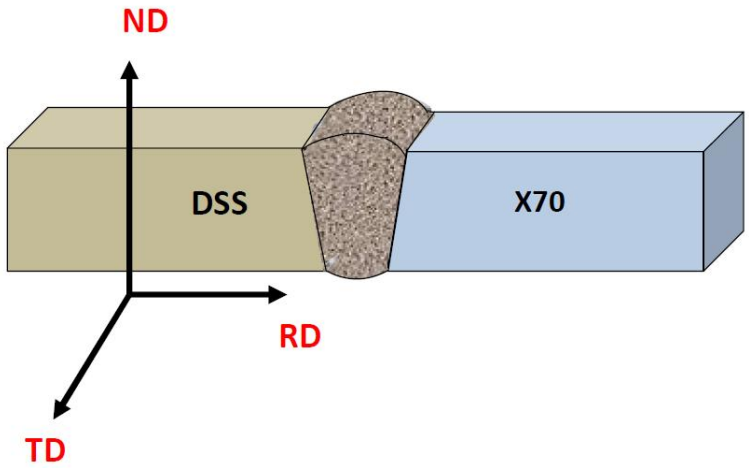

Fig. 1. Representation of the principal coordinate system in the welded joint: *Rolling Direction* (RD), *Transverse Direction* (TD), and *Normal Direction* (ND)

To study the corrosion behavior of the welded specimens, electrochemical tests were carried out in a 3.5% NaCl solution, using a Potentiostat-Galvanostat-ZRA Gamry. It is noted that the electrochemical cell is composed of three electrodes: a working electrode (the sample to be studied), an Ag/AgCl reference electrode. Its potential is the same as the potential of the saturated calomel electrode. The third electrode is a chemically inert counter-electrode, which is made of graphite. The immersion time of the samples before the electrochemical tests was 60 minutes to reach a stable potential.

Vickers hardness measurements along the weld joint were carried out using a Micro-Vickers digital hardness tester type HVS-1000 Z applying a load of 0.3 kg. The tensile test is carried out in a hydraulic universal testing machine on a circular specimen with a diameter of 8 mm and a length of 190 mm with a deformation rate of 2 mm/min. The weld is in the middle of the tensile specimen.

3. Results and Discussion

3.1 Macrostructures

Figure 2 shows the macrostructural view of the cross section of the welded joint obtained after applying several passes using two different electrodes. There is a distinction between the different passes. It can be seen that the first pass (at the bottom of the weld) is characterized by a very limited area, unlike the last pass (at the top), which is wider, which means that the dilution rate at the top is greater than at the bottom of the joint. This difference is due to the difference in heat input between the top and bottom of the joint [13].

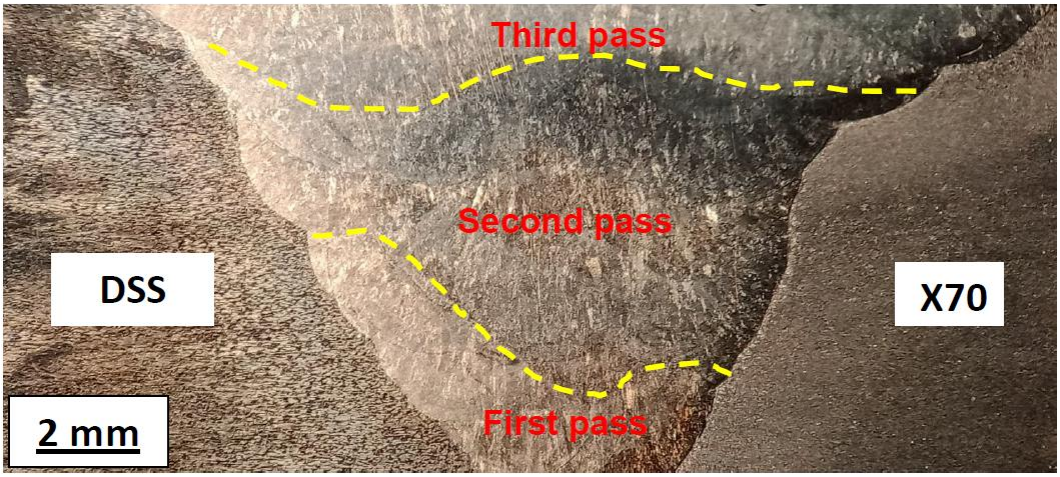

Fig. 2. Macrography of the welded joint of X70 steel assembled to duplex stainless steel by tungsten gas arc after the various passes using two different electrodes

3.2. Microstructures observations

3.2.1 Microstructure of the base metals

Figure 3 presents the microstructure of the two base metals, i.e., the X70 steel (Figure 3a) and the duplex stainless steel (Figure 3b). On one hand, the microstructure of X70 steel is composed of a ferrite matrix (Clear) containing small colonies of pearlite (Dark) distributed homogeneously. On the other hand, the microstructure of duplex stainless steel is composed of two phases (ferrite and austenite) elongated in the same direction. This direction corresponds to the direction of rolling during the manufacture of the tubes. The grain length of the two phases varied from about 100 to 200 µm.

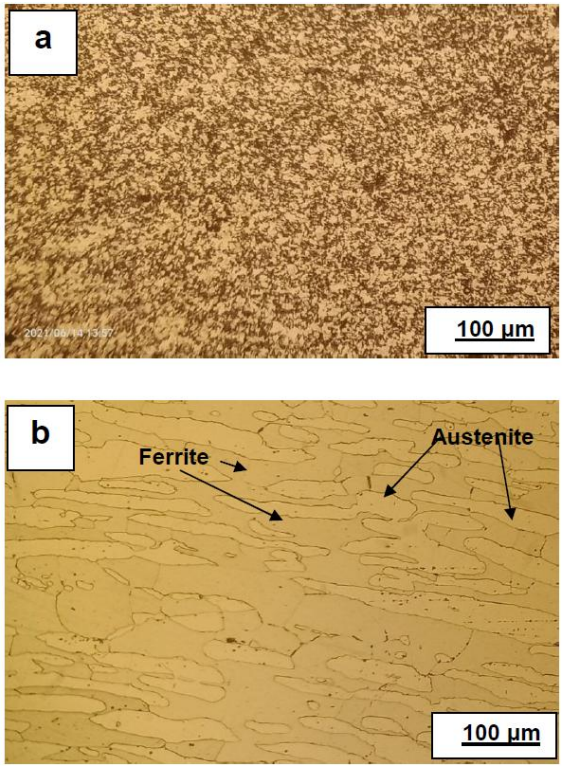

Fig. 3. Microstructure of the two base metals (a) X70 steel and (b) duplex stainless steel

The results of the EBSD analysis on DSS steel are shown in Figure 4. This figure shows the TD-IPF and phase DSS plans. The two, Figure 4a and b, show that the grains of the two phases are oriented in the rolling direction. Figure 4b shows that ferrite (green colour) and austenite (red colour) have roughly the same proportion. It was found that the DSS has a typical band microstructure of elongated grains α and γ in rolling orientation [14].

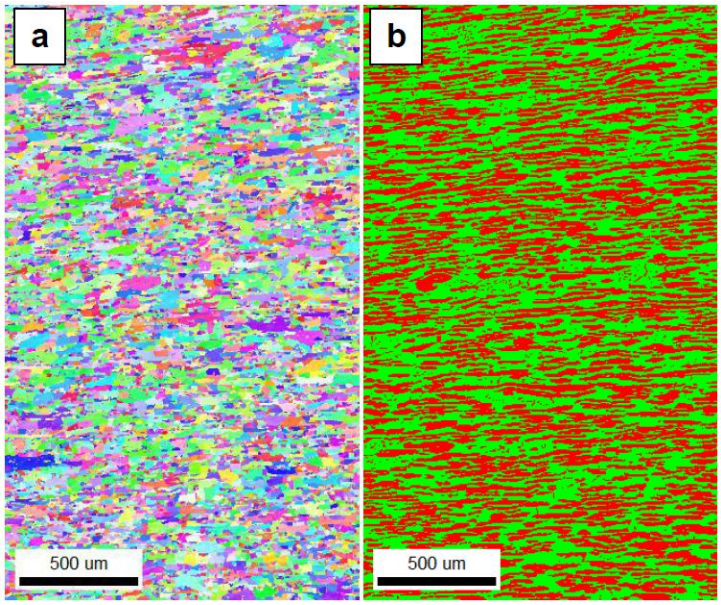

Fig. 4. (a) TD-IPF EBSD map, and (b) phase-coloured map (47% austenite in red colour, 53% ferrite in green colour) of duplex stainless steel

3.2.2. Microstructure of the welded joints

Figure 5 shows the areas where the micrographs were taken in the welded joint. This investigation will be focused on the effect of the first and the second pass on the welded joint.

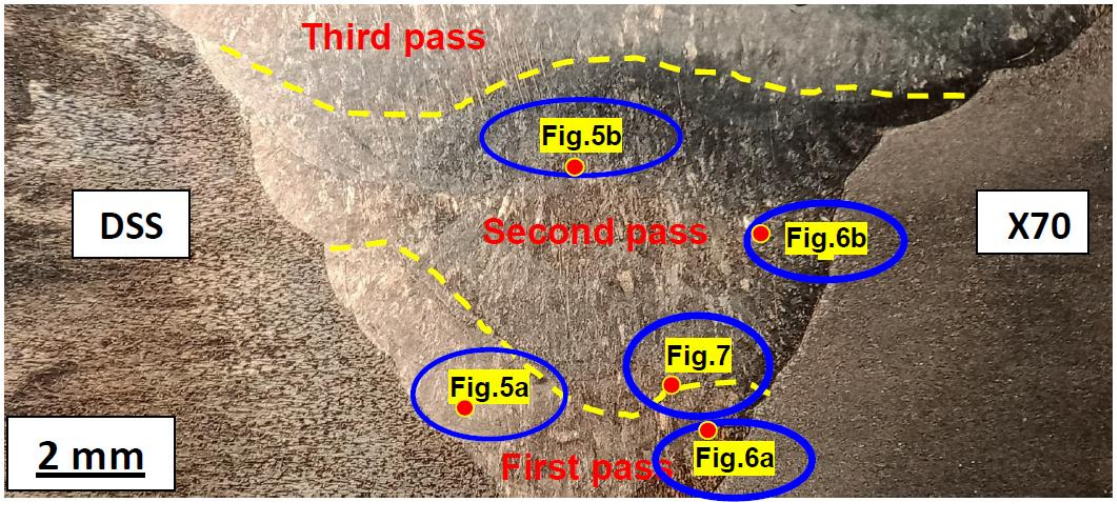

Fig. 5. Macrography of the welded joint of X70 steel assembled to duplex stainless steel by tungsten gas arc after the various passes using two different electrodes. The circles correspond to the areas where the micrographs were taken in the welded joint

Figures 6, 7, and 8 show the microstructure in the different zones of the welded joint. This first analysis will be focused on the difference in microstructure between the first and the second pass. For the fusion zone, which is the zone most affected by the use of two electrodes, Fig.6 shows the microstructure in the first and second pass. The microstructure in the first pass is characterized by different sizes and shapes of ferritic grains, as shown in Figure 6a. The microstructure in the second pass (Figure 6b) is slightly different from that of the first pass. Indeed, some grain types are similar to what was previously shown as 3, but other new areas appear with quite different ferritic grains as shown by 1 and 2. This difference in microstructure between the zones of the two passes is mainly due to different chemical compositions and the thermal effect, i.e., the first pass undergoes the heat effect of the second pass. It has been found that double pass welding leads to excessive heat input, which introduces changes to the microstructure of the FZ and even to the HAZ [15].

Figure 7 shows the heat-affected zone on the side of the X70 steel in the region of the first pass (Figure 7a) and the second pass (Figure 7b). There is not a big difference except the formation of a free zone (band devoid of pearlite) between the HAZ and the fusion zone in the region of the second pass (Figure 7b). This same observation was found by Belkessa *et al.* [16] during the study of the welding of a duplex stainless steel with a low alloy steel and which was explained by the fact that the molten metal is richer in Cr and has a strong affinity for carbon, which favours the migration of carbon from the base metal towards the fusion zone during welding. This diffusion of carbon atoms causes the formation of a narrow zone depleted in carbon atoms, 10 µm wide [11]. In addition, Boumerzoug *et al*. [17] found that chromium is an element that actively diffuses across the interface between these two same steels (X70 / DSS) bonded by a solid diffusion process.

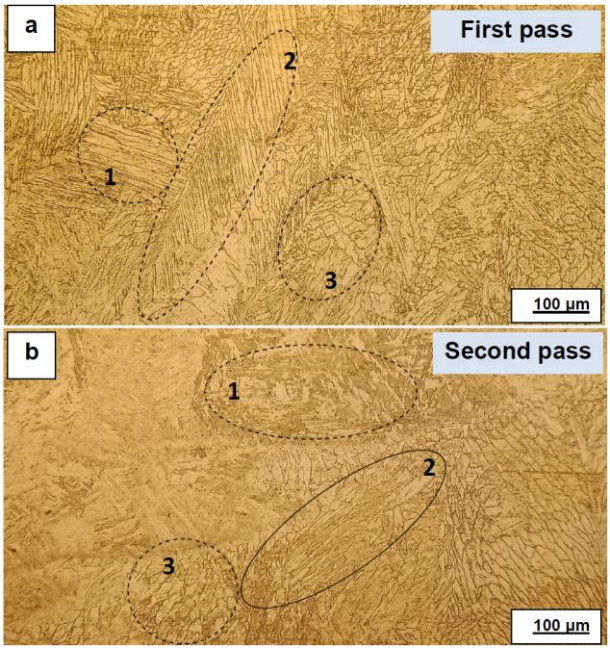

Fig. 6. Microstructure of the fusion zone in (a) the first pass and (b) the second pass of the welded joint of X70 steel assembled to duplex stainless steel by tungsten gas arc using two different electrodes for the first and the second pass, respectively

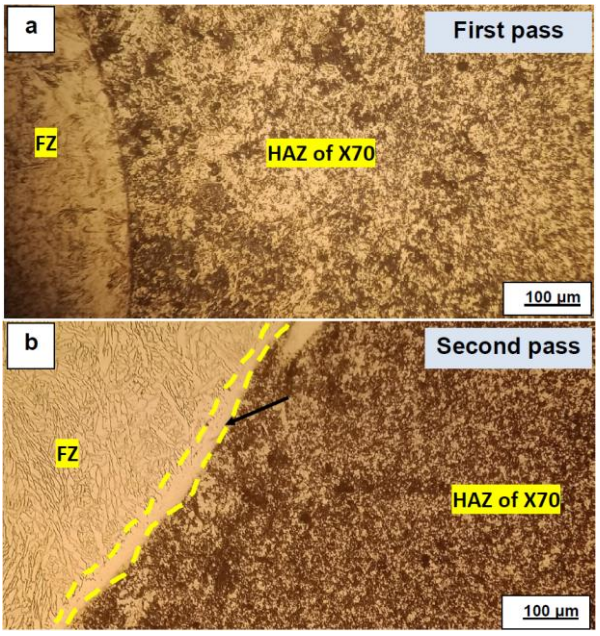

Fig. 7. Microstructure of the fusion zone in (a) the first pass and (b) the second pass of the welded joint of X70 steel assembled to duplex stainless steel by tungsten gas arc after the various passes using two different electrodes for the first and the second pass, respectively

Figure 8 shows the heat-affected zone on the side of the duplex stainless steel in the region of the first pass (Figure 8a) and the second pass (Figure 8b). It has been found that the grains of the HAZ and close to the fusion zone change orientation with a certain angle concerning their initial directions (Rolling Direction). This phenomenon is visible in the region of the second pass (Figure 8b). This behaviour is due to the thermal effect of the fusion zone on the HAZ**.**

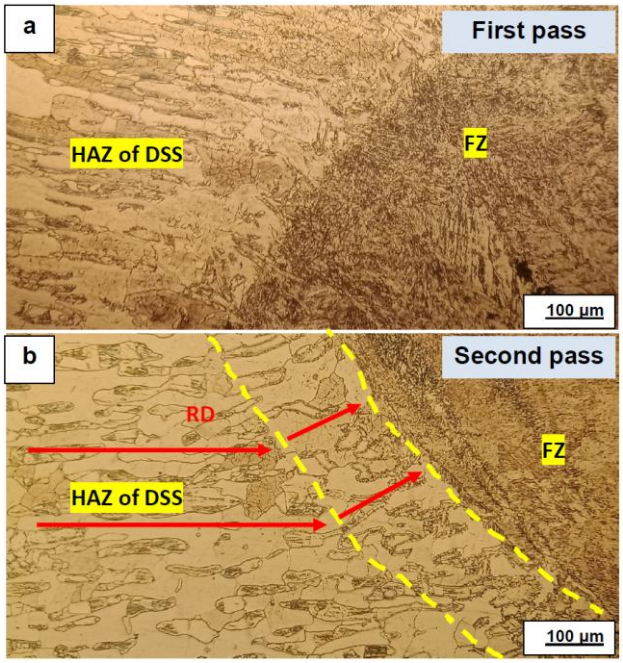

Fig. 8. Microstructure of the fusion zone in (a) the first pass and (b) the second pass of the welded joint of X70 steel assembled to duplex stainless steel by tungsten gas arc after the various passes using two different electrodes for the first and the second pass, respectively

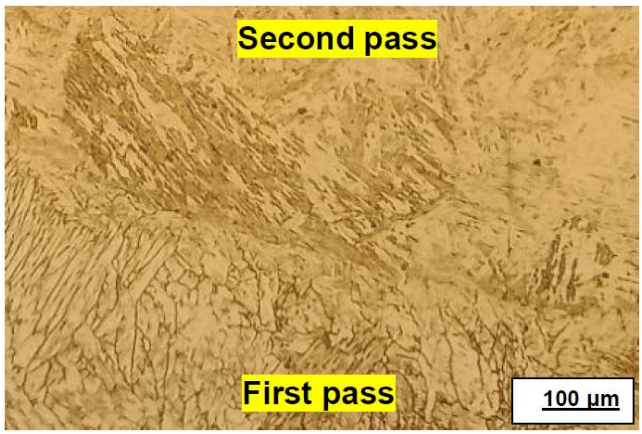

Fig. 9. Microstructure of the connection zone between the first (electrode: E2209) and second pass (Electrode: ER70S) in fusion zone of the welded joint of X70 steel assembled to duplex stainless steel by tungsten gas arc after the various passes using two different electrodes for the first and the second pass, respectively

Figure 9 shows the transition zone from the first pass to the second pass. The presence of a line that separates these two passes is observed, where the microstructure of the first pass is different from that of the second pass. This difference could be explained by the fact that the first pass undergoes the thermal effect, which comes from the deposition of the second pass, which is considered as a heat treatment application on the first pass, which induces micro-structural changes in this pass.

3.3. EBSD analysis of the welded joint

Figure 10 shows the TD-IPF EBSD map of the welded joint of X70 steel to duplex stainless steel. In this part, the main three zones corresponding to the first pass are presented: the fusion zone and the heat-affected zone of X70 steel and duplex stainless steel. First, the fusion zone consists of elongated grains with isolated areas containing fine grains, which are indicated by circles (Figure 9a and 9b). During the growth of the solid in the molten bath, the form of the solid-liquid interface controls the shape, size, and crystallographic orientation of solidification microstructures [18]. For this welded joint, the solid/liquid interface is the FZ/HAZ interface. Therefore, the formation of the elongated grains obtained in the FZ can be attributed to this interface, and which a typical solidification microstructure is as found in previous works [19-22].

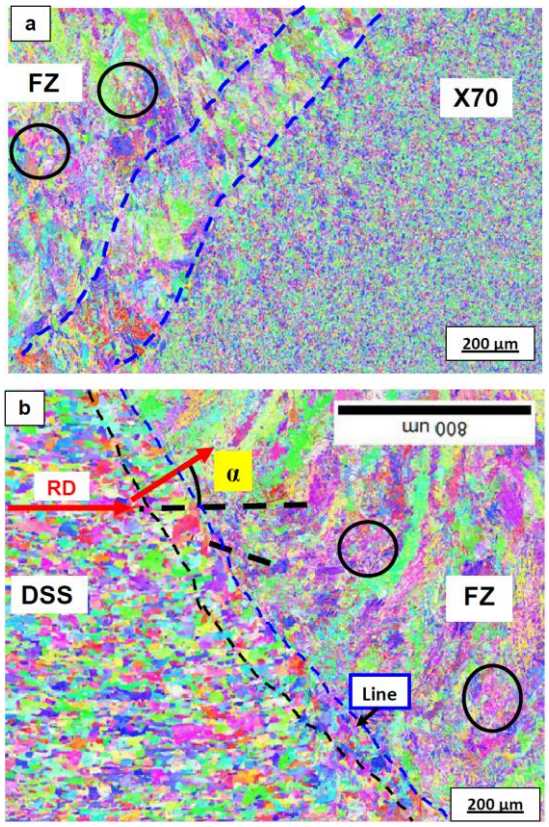

Fig. 10. TD-IPF EBSD maps in the welded joint of X70 steel joined to duplex stainless steel, showing the fusion zone with (a) the heat affected zone of X70 steel and (b) the heat affected zone of duplex stainless steel

However, the HAZ of X70 steel is fine grained (Figure 10a). The zone of intersection between the fusion zone and this heat-affected zone is a wide zone formed by non-elongated grains (delimited by two blue lines). On the other hand, there is a line that separates the heat-affected zone on the side of the duplex stainless steel from the fusion zone (Figure 10b). As mentioned in Figure 7b, similarly, it was also observed on the EBSD map of Figure 10b, the same phenomenon of change in orientation of the grains of the HAZ and close to the fusion zone of a certain angle α (~ 30°) concerning their initial directions (Rolling Direction). It should be mentioned that it is a simple rotation of the grains without a fundamental change of crystallographic orientation. It has been found that for the HAZ of welded duplex stainless steel, controlling the amount of both phases (Ferrite, Austenite) in this area will affect the corrosion resistance of the welded joint, as a high level of ferrite may to cause intergranular corrosion [23]. Additionally, it has been found that a high level of ferrite also decreases the impact resistance of the welded joint [24-26].

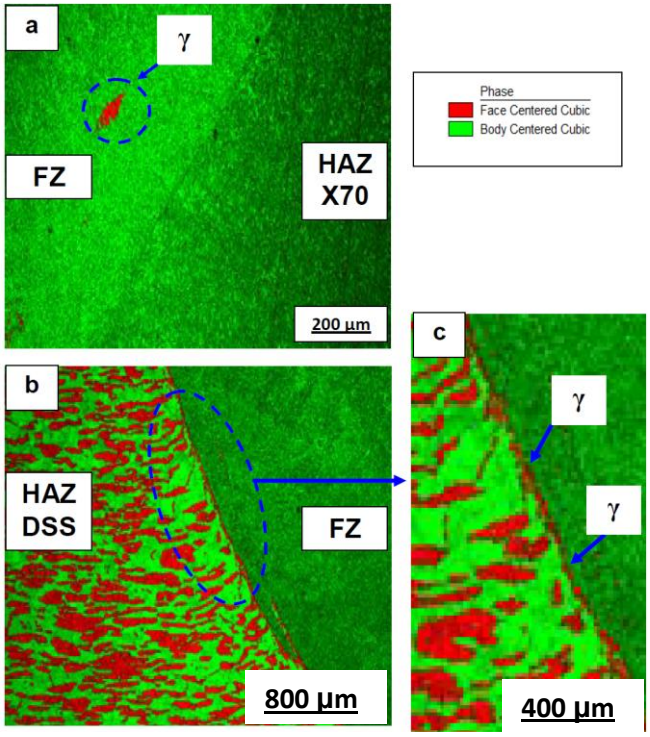

Fig. 11. Phase-coloured map (53% ferrite in green colour, 47% austenite in red colour) in the welded joint of X70 steel joined to duplex stainless steel showing the fusion zone with; (a) the heat affected zone of X70 steel and; (b) the heat affected zone of duplex stainless steel; (c) Magnification of a selected zone in the interface HAZ of DSS /FZ

Figure 11 presents the coloured phase map (austenite in red, ferrite in green) at the interface (HAZ of X70/FZ) (Figure 11a) and at the interface (FZ/HAZ of DSS). As presented in Figure 11a, the majority of the microstructure is a ferrite phase. However, an austenitic phase island is detected in FZ (indicated by a circle). This austenitic phase was formed during the solidification process. Regarding the interface (FZ/HAZ of the DSS) as shown in Figure 11b, there is a distinction between

the FZ and the HAZ of the DSS. However, a magnification of a selected area at this interface shows a small dispersed austenite phase formed at this interface (Figure 11c).

3.4. Hardness measurements

Figure 12 shows the Vickers microhardness profiles through the first and second pass of the same welded joint. The highest hardness is recorded in the fusion zone for both passes and reached the value of 290 Hv. The greater hardness value in the fusion zone can be explained by the application of two electrodes in this zone, which introduced more hardening elements existing in these two electrodes, mainly Ni, Mn, Mo, and Cr. Chromium is the most hardening element among these additional elements. It is important to mention that the ER2209 welding electrode contains 23 % Cr, i.e., richer than duplex stainless steel, which contains 20 %. The effect of Cr in the hardening of the fusion zone was also observed by Kawakami *et al.* [27], who found that Chromium increased the hardness of the fusion zone in the welded mild steel. Most of the research works have found that the FZ has the highest hardness value in the welded joint compared to other zones [28-31].

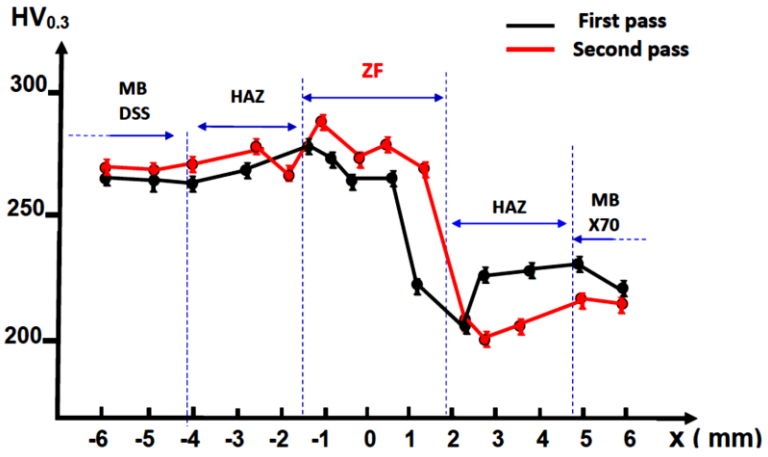

Fig. 12. Vickers microhardness profiles through the first and second pass of the weld joint of X70 steel joined to duplex stainless steel

3.5. Tensile test

Figure 13 shows the tensile test curve (Stress versus strain) obtained on a specimen of X70 steel welded to duplex stainless steel. It can be seen that this curve is typical of a classic curve because the three domains are observed, i.e., the elastic domain, the plastic domain, and finally, the rupture domain. It has been reported that despite the chemical difference between the two base metals, the choice of filler metal is among the parameters that can produce acceptable welds [4].

According to the values of tensile strength and the yield strength of the welded joint of X70 steel with duplex stainless steel, it can be concluded that the tensile strength value of the welded joint is between the values of X70 steel and duplex stainless steel, as indicated in Table 5. The maximum resistance (Tensile Strength) of the welded sample is very good since it reaches more than 96% of the nominal value of duplex stainless steel. On the other hand, the value of the yield strength of the

welded joint is higher than that of the two base metals. The increase in the yield strength can be attributed to the chemical composition of the welded joint.

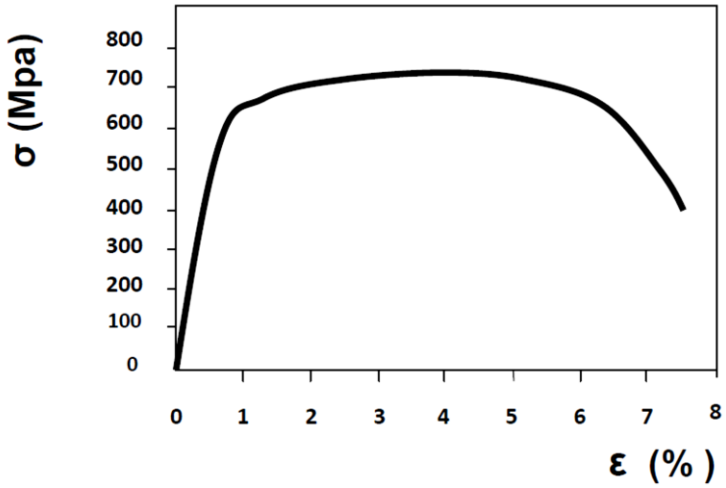

Fig. 13. Tensile test curve obtained on a specimen of X70 steel welded to duplex stainless steel

Table 5
The values of yield strength and tensile strength of the welded joint

Material	Yield Strength (MPa)		Tensile Strength (MPa)	
X70	482	[20]	565	[29]
DSS	510	[21]	750	[30]
Welded DSS/X70	662 ± 12		727 ± 14	

3.6. Corrosion test

The polarization curves of the three samples (Welded joint and the two base metals X70 and DSS), immersed in 3.5 wt. % NaCl solution is presented in Figure 14. The polarization curves show a significant shift in the corrosion potential from the most negative values to the least negative values, according to the following order: X70, welded joint, and the duplex steel. This allows us to deduce that the welded joint has a resistance to corrosion between X70 steel and duplex steel.

Figure 15 shows the macro view of the welded joint from duplex steel to X70 steel before (Figure 15a) and after immersion in a 3.5% by weight NaCl solution during 24 hrs. (Figure 15b). Figure 13b shows that the X70 steel side is more corroded than the DSS steel. It has been proven that DSS steels offer good corrosion properties even compared to some stainless steels, which increases the service life of duplex stainless-steel parts or structures made of this type of steel [32]. However, the weld is slightly corroded because it represents the fusion zone where it contains Cr-rich regions and others less. After all, two electrodes were used during the welding process.

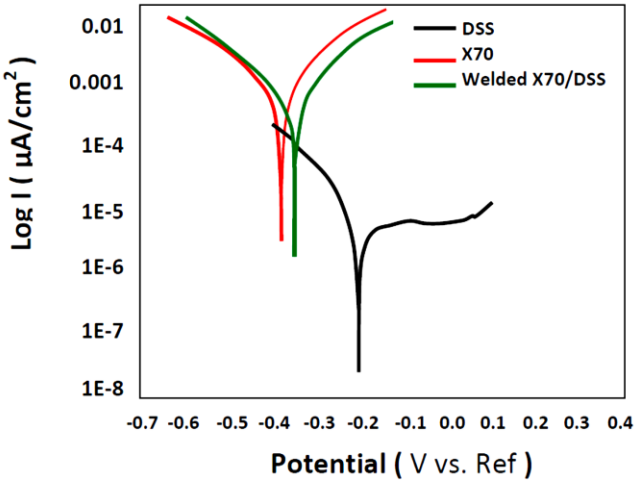

Fig. 14. Polarization curves of the welded joint, the X70 steel and the duplex steel, immersed in 3.5 wt % NaCl solution

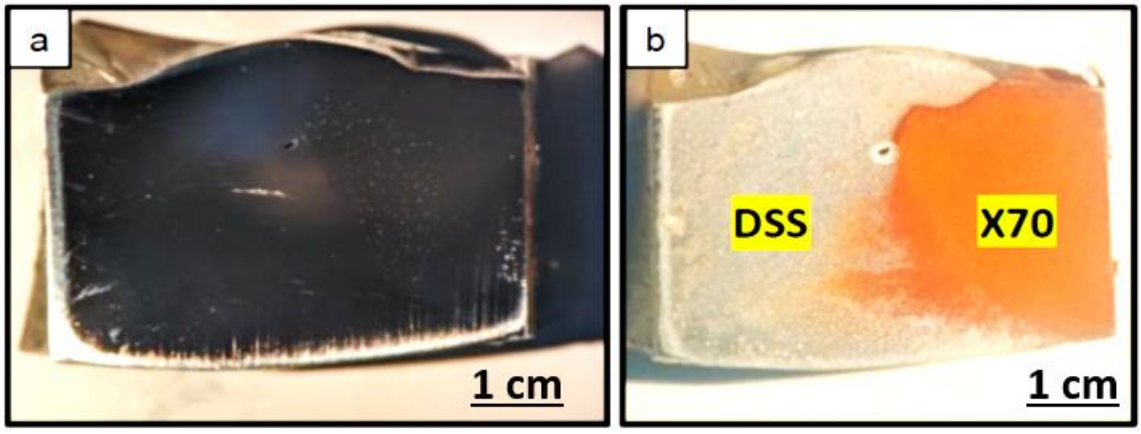

Fig. 15. Macroscopic view of the welded joint of X70 steel to the duplex steel (a): before and (b): after immersion in solution of 3.5 wt.% NaCl

4. Conclusions

This study successfully investigated the welding of low-carbon X70 steel to duplex stainless steel (DSS) using the Gas Metal Arc Welding (GMAW) process with two different filler metals applied to the same welded joint. The results showed that the microstructure of the welded joint differed between the X70 steel and DSS sides, with the X70 side exhibiting more corrosion than the DSS side. The welded joint demonstrated intermediate corrosion resistance between the two base materials. The fusion zone exhibited the highest hardness due to its chromium-rich composition. Additionally, the tensile strength of the welded joint was found to be between that of X70 steel and duplex stainless steel, while the yield strength of the welded joint exceeded that of both base metals.

References

[1] Z. Boumerzoug, F. Delaunois, O. Beziou and I. Hamdi, "Investigation of the Heat Affected Zone by Thermal Cycle Simulation Technique," The International Journal of Materials and Engineering Technology 5, 2, (2022): 80-83. https://dergipark.org.tr/en/pub/tijmet/issue/72047/869026#article_cite

[2] B. Mvola, P. Kah and J. Martikainen, "Dissimilar Ferrous Metal Welding using Advanced Gas Metal Arc Welding Processes," Reviews on Advanced Materials Science 38, (2014): 125-137. https://www.ipme.ru/e-journals/RAMS/no_23814/03_23814_mvola.pdf

[3] Y.V. Budkin, "Welding Joints in Dissimilar Metals," Welding International 25, 7, (2011): 523-525. https://doi.org/10.1080/09507116.2011.554254

[4] B. Mvola, P. Kah, J. Martikainen and R. Suoranta, "Dissimilar Welded Joints Operating in Sub-Zero Temperature Environment," The International Journal of Advanced Manufacturing Technology 87, (2016): 3619-3635. https://doi.org/10.1007/s00170-016-8711-4

[5] S. Kaewkuekool and B. Amornsin, "A Study of Parameters Affecting the Mechanical Property of Dissimilar Welding between Stainless Steel (AISI304) and Low Carbon Steel," Proceedings of the 1st WSEAS International Conference on Materials Science (2008): 105-109. https://dl.acm.org/doi/10.5555/1984059.1984081

[6] B.I. Mendoza, Z.C. Maldonado, H.A. Albiter and P.E. Robles, "Dissimilar Welding of Superduplex Stainless Steel/HSLA Steel For Offshore Applications Joined By GTAW," Engineering 2, 7, (2010): 520-528. https://doi.org/10.4236/eng.2010.27069

[7] S.M. Zahraei, R. Dehmolaei and A. Ashrafi, "The Effect of Heat Input on Microstructure and HAZ Expansion in Dissimilar Joints between API5L X80 / DSS 2205 Steels Using Thermal Cycles," Revista de Metalurgia 58, 2, (2022): e222. https://doi.org/10.3989/revmetalm.222

[8] N.A. McPherson, K. Chi, M.S. Mclean and T.N. Baker, "Structure and Properties of Carbon Steel to Duplex Stainless Steel Submerged Arc Welds," Materials Science and Technology 19, 2, (2003): 219-226. https://doi.org/10.1179/026708303225009643

[9] J. Wang, M.-X. Lu, L. Zhang, W. Chang, L.-N. Xu and L.-H. Hu, "Effect of Welding Process on the Microstructure and Properties of Dissimilar Weld Joints between Low Alloy Steel and Duplex Stainless Steel," International Journal of Minerals, Metallurgy, and Materials 19, 6, (2012): 518-524. https://doi.org/10.1007/s12613-012-0589-z

[10] M.Puchianu, H.F. Daşcău and G. Solomon, "Studies Regarding FCAW Welding of Dissimilar Joints Between Duplex Stainless Steel and Naval Carbon Steel," Defect and Diffusion Forum 416, (2022):43–54. https://doi.org/10.4028/p-i26fn3

[11] A. Eghlimi, M. Shamanian, M. Eskandarian, A. Zabolian, M. Nezakat and J.A. Szpunar, "Evaluation of Microstructure and Texture Across the Welded Interface of Super Duplex Stainless Steel and High Strength Low Alloy Steel," Surface and Coatings Technology 264, (2015): 150-162. https://doi.org/10.1016/j.surfcoat.2014.12.060

[12] O. Beziou, I. Hamdi, Z. Boumerzoug, F. Brisset and T. Baudin, "Effect of Heat Treatment on the Welded Joint of X70 Steel Joined to Duplex Stainless Steel by Gas Tungsten Arc Welding," The International Journal of Advanced Manufacturing Technology 127, (2023):2799–2814. https://doi.org/10.1007/s00170-023-11675-9

[13] R. Cervo, P. Ferro, and A. Tiziani, "Annealing Temperature Effects on Super Duplex Stainless Steel UNS S32750 Welded Joints. I: Microstructure and Partitioning of Elements," Journal of Materials Science 45, (2010): 4369–4377. https://doi.org/10.1007/s10853-010-4310-1

[14] M. Wang, H. Li, Y. Tian, H. Guo, X. Fang and Y. Guo, "Evolution of grain interfaces in annealed duplex stainless steel after parallel cross rolling and direct rolling," Materials 11, 5, (2015):816. https://doi.org/10.3390/ma11050816

[15] V.A. Hosseini, K. Hurtig and L. Karlsson, "Bead by Bead Study of a Multipass Shielded Metal Arc-Welded Super-Duplex Stainless Steel," Weld in the World 64, (2020): 283–299. https://doi.org/10.1007/s40194-019-00829-7

[16] B. Belkessa, D. Miroud, B. Cheniti, N. Ouali, M. Hakem and M. Djama, "Dissimilar Welding Between 2205 Duplex Stainless Steel and API X52 High Strength Low Alloy Steel," Diffusion Foundation 18, (2018): 7–13. https://doi.org/10.4028/www.scientific.net/DF.18.7

[17] Z. Boumerzoug, L. Baghdadi, F. Brisset, D.Solas and T. Baudin, "Solid-State Diffusion Bonding of X70 Steel to Duplex Stainless Steel," Acta Metallurgica Slovaca 28, 2, (2022): 106-112. https://doi.org/10.36547/ams.28.2.1504

[18] S.A. David, S.S. Babu, and J.M. Vitek, "Welding: Solidification and microstructure," JOM 55, (2003): 14-20. https://doi.org/10.1007/s11837-003-0134-7

[19] A.F. Norman, I. Brough and P.B. Prangnell, "High Resolution EBSD Analysis of the Grain Structure in an AA2024 Friction Stir Weld," Materials Science Forum 331-337 (2000): 1731-1718. https://doi.org/10.4028/www.scientific.net/MSF.331-337.1713

[20] S. Babu, H.K.D.H. Bhadeshia and L.-E. Svenson, "Crystallographic Texture and the Austenite Grain Structure of Low Alloy Steel Weld Deposits," Journal of Materials Science Letters 10, (1991):142-144. https://doi.org/10.1007/BF02352829

[21] S. Hamza, Z. Boumerzoug, A.-L. Helbert, F. Bresset and T. Baudin, "Texture analysis of Welded 304L Pipeline Steel," Journal of Metals, Materials and Minerals 29, 3, (2019). https://jmmm.material.chula.ac.th/index.php/jmmm/article/view/524

[22] Z. Boumerzoug, N. Cherifi and T. Baudin, "Texture in Welded Industrial Aluminium," Applied Mechanics and Materials Research 563, (2014): 7-12. https://doi.org/10.4028/www.scientific.net/AMM.563.7

[23] Liu, Xin, Yulong Hu and Nian Liu, "Effect of Welding Current on Corrosion Resistance of Heat-Affected Zones of HDR Duplex Stainless Steel," Materials 17, no. 9 (April 25, 2024): 1986. https://doi.org/10.3390/ma17091986

[24] Dong, Zhihai, Yiwen Li, Boyoung Lee, Aleksandr Babkin and Yunlong Chang, "Research Status of Welding Technology of Ferritic Stainless Steel," The International Journal of Advanced Manufacturing Technology 118, no. 9–10 (October 9, 2021): 2805–31. https://doi.org/10.1007/s00170-021-08128-6

[25] Higelin, Anne, Sandra Le Manchet, Gilles Passot, Sarata Cissé and John Grocki, "Heat-affected Zone Ferrite Content Control of a Duplex Stainless Steel Grade to Enhance Weldability," Welding in the World 66, no. 8 (June 29, 2022): 1503–19. https://doi.org/10.1007/s40194-022-01326-0

[26] Westin, E. M. and L. G. Westerberg, "Evaluation of Methods Used for Simulation of Heat-affected Zones in Duplex Stainless Steels," Welding in the World 68, no. 8 (February 23, 2024): 1941–63. https://doi.org/10.1007/s40194-024-01698-5

[27] H. Kawakami, H. Kuno, Y. Kawahito and H. Wang, "Hardness Enhancement by Molten Metal Flow in Laser Remelting with an Ultra-Thin Additional Element Coating," Journal of Materials Processing Technology 288, (2021): 116888. https://doi.org/10.1016/j.jmatprotec.2020.116888

[28] N. Charde, "Microstructure and Fatigue Properties of Dissimilar Spot Welds Joints of AISI 304 and AISI 1008," International Journal of Automotive and Mechanical Engineering 7, (2022): 882–899. https://doi.org/10.15282/ijame.7.2012.7.0072

[29] T.N. Le, A.T. Vu, H.C. Le, V.H. Dong, V.P. Nguyen and T.N. Dang, "Effect of Heat Source on the Formation of Welding Zone Structure Between Carbon Steel and Stainless Steel Applied in Shipbuilding," International Journal of Advanced Science, Engineering and Information Technology 14, 2, (2024):749–760. https://doi.org/10.18517/ijaseit.14.2.18828

[30] N. Sankar, S. Malarvizhi and V. Balasubramanian, "Mechanical Properties and Microstructural Characteristics of Rotating Arc-Gas Metal Arc Welded Carbon Steel Joints," Journal of the Mechanical Behavior of Materials 30, 1, (2021): 49-58. https://doi.org/10.1515/jmbm-2021-0006

[31] S. Wu, W. Xiao, L. Gong and F. Zhang, "Comparison of Microstructure and Mechanical Properties of Ultra-Narrow Gap Metal Active Gas Arc Welded and Narrow Gap Submerged Arc Welded Q235A Low Carbon Steel," Materials 16, 19, (2023): 6601. https://doi.org/10.3390/ma16196601

[32] Songging Wen, "Metallurgical Evaluation of Cast Duplex Stainless Steels and Their Weldments," (MSc Thesis, The University of Tennessee Knoxville, 2001).